Journal of Engineering Science and Technology
Vol. 13, No. 5 (2018) 1396 - 1410

U-SHAPED SLOTS LOADED PATCH ANTENNA WITH DEFECTED GROUND PLANE FOR MULTIBAND MODERN COMMUNICATION SYSTEMS

K. G. JANGID[1,*], P. K. JAIN[2], NEELAM CHOUDHARY[2], BRAJRAJ SHARMA[3], V. K. SAXENA[2], V. S. KULHAR[1], D. BHATNAGAR[2]

[1]Department of Physics, Manipal University, 303007, Jaipur, India
[2]Microwave Lab, University of Rajasthan, 302004, Jaipur, India
[3]Department of Physics, SKITM & G, 302017, Jaipur, India
*Corresponding Author: kgkris1980@rediffmail.com

Abstract

In this article, the design and performance of circular radiating patch element with two U-shaped slots and defected ground plane, comprising of a triangular notch monopole structure with rhomboid shape resonator, is reported. The proposed multiband antenna has a compact structure design for GSM 1800 MHz, WLAN, WiMAX and UWB communication systems. The antenna is designed on FR4 glass epoxy substrate of size 39 mm × 34 mm × 1.59 mm by using computer simulation tool CST Microwave Studio 2014. For confirmation of simulation results, prototypes are fabricated and their performance is tested in free space. Measured results demonstrate that fabricated antenna provides triple bands with impedance bandwidth of 157 MHz (1.733 GHz to 1.89 GHz), 3.2 GHz (2.29 GHz to 5.49 GHz) & 10.45 GHz (6.83 GHz to 17.28 GHz), almost flat high gain between 4 to 6 dBi and good radiation patterns in the desired frequency range. The maximum measured gain of proposed structure is close to 6.59 dBi at 4.40 GHz. The circular polarization is also realized in the frequency range 4.12 GHz to 5.20 GHz with axial impedance bandwidth 1.08 GHz. The specific absorption rate SAR values of proposed design are also evaluated at various frequency spots which are well within the SAR values specified by the FCC. Proposed design may be proved a useful structure for advance radio communications systems as well as for the present requirements in defence applications.

Keywords: Double U-shaped slots, Monopole structure, Multiband patch antenna, Rhomboid shape resonator, Specific absorption rate, UWB communication system, WLAN.

Nomenclatures

f_{res}	Resonance frequency, GHz/MHz
h	Height of substrate, mm
m	Radial mode number
n	Angular mode number
R	Physical radius of the proposed design, mm
R_e	Effective radius of the proposed design, mm
S_{11}	Reflection coefficient, dB
TM	Transverse magnetic mode

Greek Symbols

ε_{eff}	Effective dielectric constant
ε_r	Relative permittivity
υ_0	Speed of light in free space, m/s
χ'_{mn}	n^{th} zero root derivative of Bessel function of order m

Abbreviations

GSM	Global system for mobile
UWB	Ultra wide band
WiMAX	Wireless worldwide interoperability access
WLAN	Wireless local area network

1. Introduction

For enhancing the overall performance of portable communication devices, compact size antennas are in great demand because they may be integrated easily with other circuit elements and are capable in multiband operation.

The IEEE proposed various license free spectrum bands under 802.11 WLAN and 802.16 WiMAX standards. Under WLAN standards, three bands namely 2.4 GHz (2.40-2.48 GHz), 5.2 GHz (5.15-5.35 GHz) and 5.8 GHz (5.725-5.825 GHz) are allocated while under WiMAX standards, three licensed bands namely 2.3 GHz (2.30-2.40 GHz), 2.5 GHz (2.495-2.69 GHz) and 3.5 GHz (3.50-3.60 GHz) are allocated. Planar antennas are interesting candidates for these communication applications [1, 2]. In antenna designs, wide or multiband operation can be attained through alternations in the patch structure as well as in ground plane by creating several resonance modes. Introduction of ground slots or monopole structures produces some sort of disruption that changes the path of the electrical current, which in turn increases the electrical dimensions of the ground plane.

This solid pairing between radiator and the ground slots provides a multiband operation. Extensive efforts have been made by researchers for the design and development of multiband antennas for application in mobile and wireless communication systems. These include, design of H-shaped slot antenna for multiband operation [3], X-shaped slit loaded rectangular patch [4], a simple printed monopole slot antenna with two parasitic shorted strips [5], Y-shaped monopole slot antenna [6], a square cylindrical monopole antenna with cross-shaped metal plate [7], dual band antenna with omni directional radiation pattern [8], broadband L-shaped microstrip patch antenna [9], compact dual band hook-shaped antenna [10], symmetrical L-slot antenna for triple frequency bands of

2.34–2.82 GHz, 3.16–4.06 GHz, and 4.69–5.37 GHz [11], square spiral patch for multiband operation [12], meandered shaped monopole antenna with asymmetrical ground plane [13], a tri-band microstrip slot antenna for WLAN/WiMAX application [14], ground strip with an L-shaped open slot [15], a circular radiating slot antenna for UWB communication [16], a monopole antenna with two split ring resonator pairs [17], co-planar wave guide feed patch antenna for multi-band communication systems [18], a compact annular ring shaped patch antenna with L-slot [19]. SAR (Specific absorption rate) value is also very important parameter of these multiband antennas. SAR defines the power absorption value by human body tissue [20]. The safety limits of the SAR values for portable devices are specified by the FCC.

In this article, the design and execution of a compact triple band circular patch antenna having dual U-shaped slots on top and a rhomboid type resonator along with a triangular notch on bottom side of antenna is proposed to achieve multiband operation and improved gain. The finite integration technique based computer simulation tool CST Microwave Studio™ [21] is utilized for the simulation analysis of antennas while measurements of fabricated prototypes are carried out by using R & S make Vector Network analyser model ZVA 40. The main advantage of proposed single element multiband antenna is its ability to support four applications at a time i.e. GSM 1800, WLAN, WiMAX, UWB applications with distinctly different radiation patterns, low SAR value and high gain results. A comparison between the performances of different antenna structures developed in recent times with our proposed structure is presented in Table 1. It is shown that the proposed structure is the most compact structure and provides four desired frequency bands. In the later part of this paper, design and execution of intended antenna is presented through simulated and measured results.

Table 1. Comparison of functioning of the proposed antenna with other recorded antenna.

Reference	Size (mm^2)	Operating frequency bands (GHz)	Remarks
[4]	44×46	2.37-7.89	Overall size is large
[5]	60×60	1.55-1.57, 2.395-2.695, 4.975-5.935	Overall size is very large
[6]	36×26	2.33-2.49, 4.30-10.18	Dual bands present
[7]	60×115	0.800-1.300, 1.710-2.325	Overall size is very large
[9]	40×10	2.38-2.52, 3.40-3.62	Few useful frequency bands
[14]	67×38	0.863-1.049, 1.49-2.81	Overall large size and lower band exist
Proposed Antenna	39×34	1.733-1.89, 2.29-5.49, 6.83-17.28	Compact and Cover all communication bands

2. Antenna Design and Analysis

The geometrical parameters of the circular shape patch antenna are shown in Fig. 1(a) and model of fabricated antenna is shown in Fig. 1(b). The antenna is fabricated on available glass epoxy FR-4 material. The comprehensive size of considered design is 39 mm x 34 mm. The structure is placed in the x-y plane and perpendicular direction is parallel to z-axis. The radiating element and strip feed line are engraved on top side of the dielectric material to obtain 50-ohm characteristic impedance. The partial ground plane is fabricated on bottom side of antenna. The resonance frequency of conventional circular patch with finite ground plane is obtained through the relation [22]:

$$(f_r)_{mn0} = \frac{\chi'_{mn}\upsilon_0}{2\pi R\sqrt{\varepsilon_r}} \tag{1}$$

where χ'_{mn} represents the nth zero root derivative of Bessel function of order m; (ε_r) is the dielectric constant of the substrate material; υ_0 is the speed of light in free space and 'R' is the physical radius of the proposed antenna. This resonant frequency does not consider the fringing effect. The size of the patch is electrically large due to this effect and a correction is introduced by considering an effective radius 'R_e' which replace the actual physical radius 'R' in above Eq. (1).

$$(f_r)_{mn0} = \frac{\chi'_{mn}\upsilon_0}{2\pi R_e\sqrt{\varepsilon_r}} \tag{2}$$

$$R_e = R\left\{1+\frac{2h}{\pi R\varepsilon_r}\left[\ln\frac{\pi R}{2h}+1.7726\right]\right\}^{1/2} \tag{3}$$

The optimized dimensions of the intended antenna through simulation software are: L = 39 mm, W = 34 mm, L_g = 7 mm, R = 14 mm, L_f = 8 mm, W_f = 4 mm.

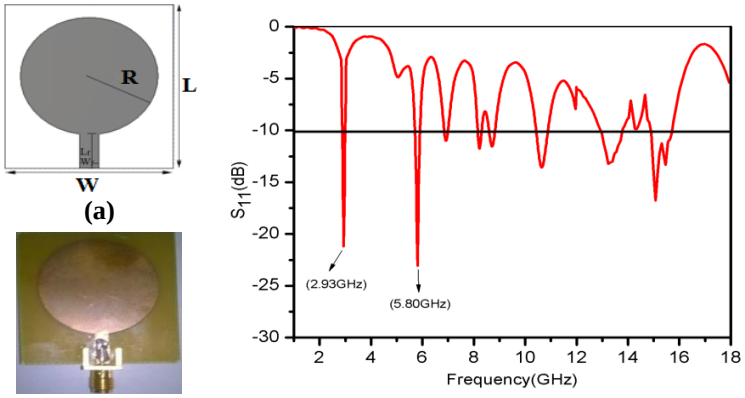

Fig. 1(a). Geometrical parameters of circular patch antenna, (b) Prototype of fabricated circular patch antenna, (c) Simulated variation of S_{11}(dB) with frequency.

The computed resonance frequencies of circular patch antenna with finite ground plane corresponding to its dominant TM_{11} mode and other excited modes TM_{21}, TM_{01} are 2.89 GHz, 4.79 GHz and 6.02 GHz respectively. This antenna matches well with the applied feed line at frequencies 2.93 GHz and 5.80 GHz, as shown in Fig. 1(c). A good agreement between simulated and calculated frequencies of this conventional circular microstrip patch antenna structure (CMPA) is detected. The simulated bandwidth of this finite ground plane structure is very narrow and maximum gain of this antenna is close to 1.02 dBi. This antenna is further modified in different steps to enhance its overall performance. In the next section, the details of applied modifications in the ground geometry and obtained results based on these modifications are reported.

2.1. Modification in ground plane

The ground plane of antenna is modified in steps which are depicted below in Figs. 2(a) to (c). The surface current distributions in all three considered cases are also shown in Figs. 3(a) to (f). The size of ground plane is optimized through CST simulation software 2014 and finally considered size of ground is 34.0 mm × 7.0 mm. This monopole structure can be considered as a patch antenna on a very thick substrate. The lower band edge frequency (f_{lb}) corresponding to S_{11}= -10 dB or VSWR= 2 of this monopole structure may be obtained following Eq. (4)

$$f_{lb} = \frac{c}{\lambda} = \frac{72}{l + r + g} \text{ (GHz)} \tag{4}$$

Here ‘l’ is the height, ‘g’ is the gap between radiating patch and ground plane, and ‘r’ is the radius of cylindrical monopole patch. For circular monopole case, the values l and r of the equivalent cylindrical monopole antenna are given by:

l = 2R, r = R/4 and hence f_{lb} will be modified to

$$f_{lb} = \frac{c}{\lambda} = \frac{72}{2R + \frac{R}{4} + g} \text{ (GHz)} \tag{5}$$

The value of ‘R’ and ‘g’ for the present case are taken as 14 mm and 1 mm respectively. The calculated lower edge frequency of this monopole structure, which has shown in Fig. 2(a), comes out to be 2.22 GHz.

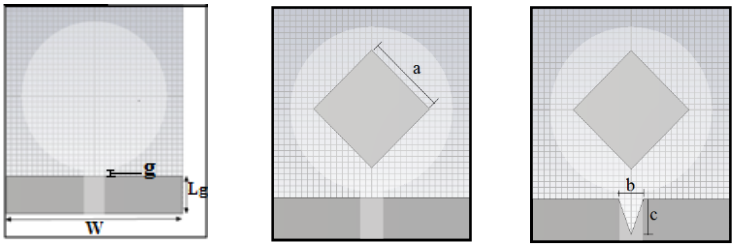

(a) **(b)** **(c)**

Fig. 2. Modified ground plane in three considered steps.

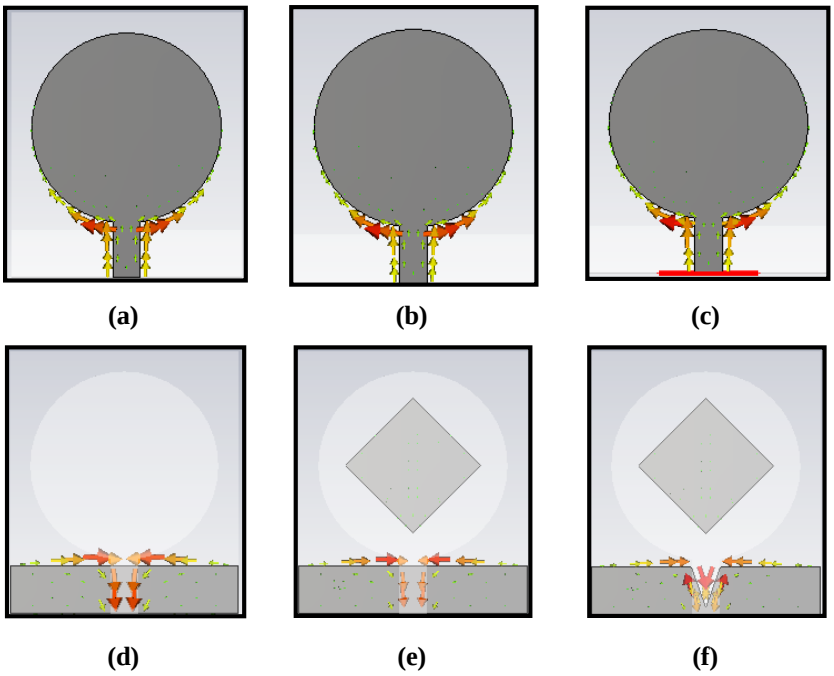

Fig. 3. Surface current distributions in various considered cases.

Wider bandwidth is interpreted in terms of various higher order modes excited in circular patch structure. Modes of the circular resonator (characterized by the roots of the derivative of the Bessel function) are closely spaced. All higher modes have a large bandwidth because the radiating patch is in the air; hence, variation in input impedance from one mode to another mode is very small. The resonant frequencies of different higher order modes (TM_{11}, TM_{21}, TM_{02}, TM_{12} and other modes) may be obtained through relations given below:

$$(f_r)_{mn0} = \frac{\chi'_{mn} \upsilon_0}{2\pi R_e \sqrt{\varepsilon_{eff}}} \tag{6}$$

$$R_e = R\left\{1 + \frac{2h}{\pi R \varepsilon_{eff}}\left[\ln\frac{\pi R}{2h} + 1.7726\right]\right\}^{1/2} \tag{7}$$

where (ε_{eff}) is the effective dielectric constant which includes the effect of monopole structure (dielectric constant of substrate material (FR-4) and beyond this substrate very thick air layer).

In the next step of modification, a rhomboid shape resonator and a triangular notch are introduced in ground plane of structure. The details of geometrical parameters of this design are included in Table 2. In each stage of modifications, antenna parameters were carefully examined. Comparison of variation of simulated S_{11} parameters with frequency for three considered steps of modification in ground plane are shown in Fig. 4. A triangular notch in the ground plane can be considered similar to a sleeve in the sleeve monopole antenna [23]. This notch provides a

particular resonant mode depending upon the dimension of this corrugation. By properly selecting the height of considered notch, an additional resonant mode at frequency 11.33 GHz as shown in Fig. 4 is achieved. The presence of dual resonance modes provides a broadband performance. With these modifications, matching of antenna with feed line at frequency 3.0 GHz is almost unaltered. Nice matching between radiating element and feed are also realized at frequencies 4.42 GHz, 9.25 GHz, 11.33 GHz, and 16.09 GHz. The simulated impedance bandwidth of antenna with defected ground structure, as shown in Fig. 2(c), is close to 12.98 GHz which is dispersed in three frequency bands 2.48-4.95 GHz, 7.14-13.03 GHz, and 13.43-18.05 GHz. Figure 10 depicts the variation of realized simulated gain with frequency. The maximum realized simulated gain of this antenna in present structure is close to 4.34 dBi, which is better than that of a monopole patch antenna structure (3.39 dBi), shown in Fig. 2(a). A rhomboid shaped resonator provides ground shielding and increases the gain of this antenna structure.

Table 2. Optimized dimensions of defected ground plane.

Geometrical Parameter	Value(mm)
Modified ground plane (L_g×W)	34.0 mm×7.0 mm
Length/width of the rhomboid shape resonator(a)	10.0 mm
Base length of the triangular notch (b)	5.0 mm
Height of the triangular notch (c)	6.0 mm

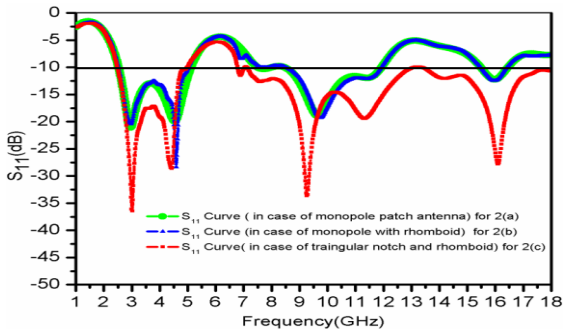

Fig. 4. Simulated variation of S_{11} (dB) with frequency in different cases.

2.2. Modification in patch geometry

For achieving the improved performance from this antenna geometry, the patch geometry shown in Fig. 2(c); is further modified in steps. The geometrical and fabricated front and back views of modified patch antenna are shown in Fig. 5. The geometrical parameters of modified patch are included in Table 3. Figure 6 illustrates the simulated surface current distributions of the proposed structure under different cases i.e. (i) when U-slot (a) is present; (ii) when U-slot (b) is present; (iii) when both U-slots are present.

Table 3. Optimized dimensions of defected patch structure.

Geometrical Parameter	Value(mm)
U slot(a) in patch (L_a×W_a)	9.5 mm×20.0 mm
U slot(b) in patch(L_b×W_b)	8.0 mm×5.2 mm
U slot width (S_w)	1.0 mm

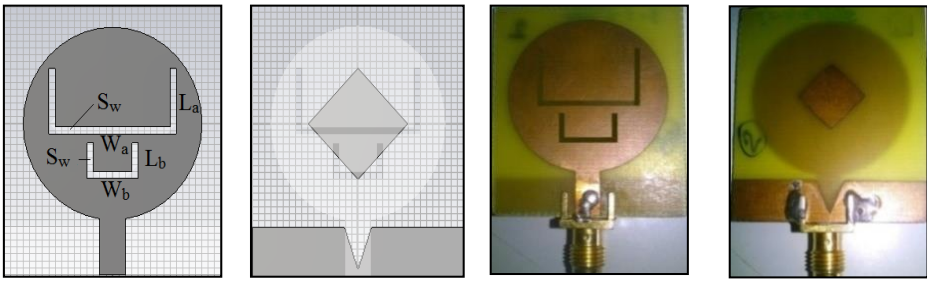

Fig. 5. Front & back views of proposed patch antenna (geometrical as well as fabricated model).

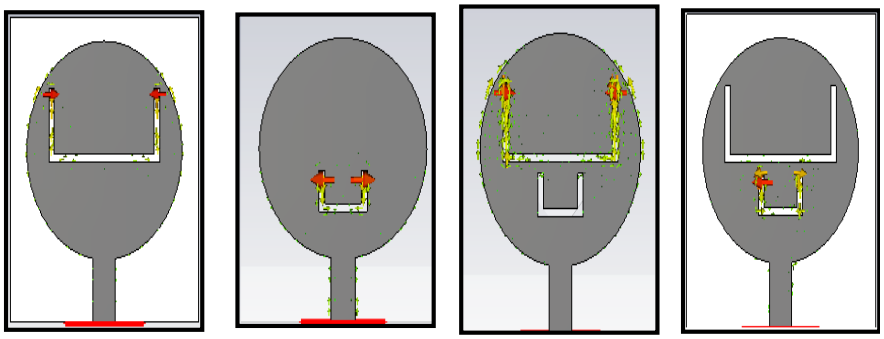

(i) 1.76 GHz **(ii) 5.57 GHz** **(iii) 1.76 GHz & 5.30 GHz**

Fig. 6. Surface current distributions in three considered cases (i) U slot (a) is present (ii) U slot (b) is present (iii) Both U slots are present.

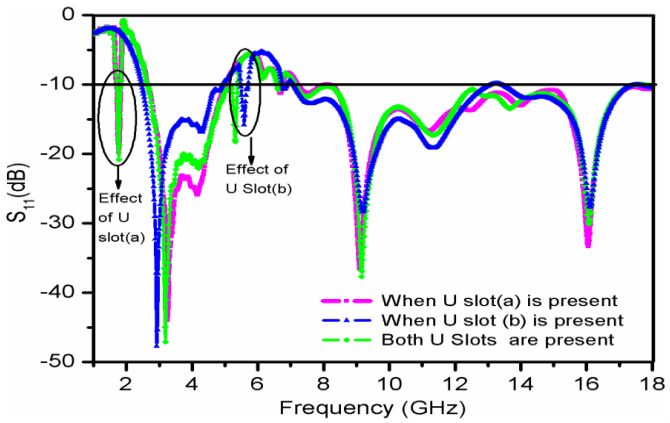

Fig. 7. Comparison between simulated reflection coefficients with frequency in different cases of inserted slots.

3. Results and Discussion

After extensive optimizations, the prototype of antenna showing triple band performance is developed and the design parameters of this prototype are listed in Tables 2 and 3. The measured and simulation results of reflection coefficient S_{11} are shown in Fig. 8. The measured results are obtained through R & S make Vector network analyser (ZVA 40). The measured results shown in Fig. 8 provide a wide impedance bandwidth extended between frequency range 2.29 GHz to 17.28 GHz for S_{11} < -10 dB, with rejection band lying in frequency range 5.49 GHz - 6.83 GHz for S_{11}> -10 dB. The presence of higher order modes due to monopole structure and triangular notch in ground plane significantly contributes in the enhancement of impedance bandwidth. An additional frequency band spread in between 1.733 GHz to 1.89 GHz frequency range is also realized. Measured results also demonstrate a nice matching between radiating element and feed at frequencies 1.81 GHz, 3.00 GHz, 4.22 GHz, 7.33 GHz, 9.34 GHz and 14.24 GHz. A reasonable agreement between experimental and simulated results is realized. The minor deviation between simulated and experimental results is perhaps due to fabrication error and associated measurement limitations.

Figures 9(a) and (d) illustrate the simulated surface current distribution of the proposed structure at 1.76 GHz and 5.30 GHz. The maximum current density appears mainly along the U-shaped slots at the patch, which are responsible for first (1.76 GHz), and third (5.30 GHz) resonance frequencies. Inserted U-shaped slots on patch corresponding to these frequencies are working as individual leaky resonators and maximum currents on the patch are flowing along the outer and inner edges of the slots [24]. The surface currents are more centralized around the slots in the structure and hence for each introduced slot; a resonant frequency band is generated. These frequency bands are useful for GSM 1800 MHz and WLAN/WiMAX communication systems. Figures 9(b) and (e) indicate that the maximum surface currents mostly centralize near the feed line and radiation patch. The triangular notch in ground plane is responsible for resonance frequencies 3.18 GHz & 9.15 GHz, which are depicted in Figs. 9(c) and (f). A comparison of gain performance of antenna in different situation is shown in Fig. 10. On introducing a rhomboid shape resonator in bottom side of antenna, an increase in gain of antenna in lower frequency band may be obtained. The maximum measured gain of antenna is approximate 6.59 dBi at 4.40 GHz which is shown in Fig. 11.

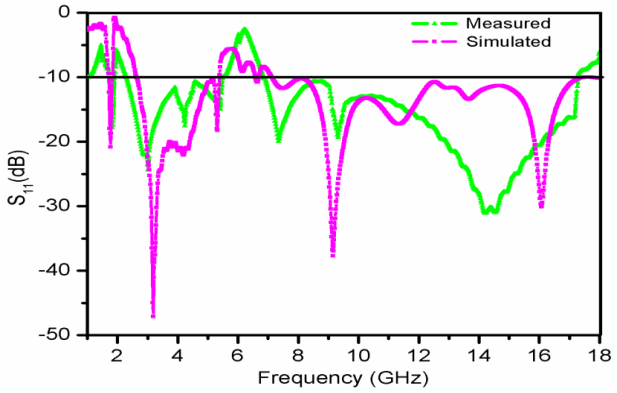

Fig. 8. Measured and Simulated variation of S_{11} (dB) with frequency.

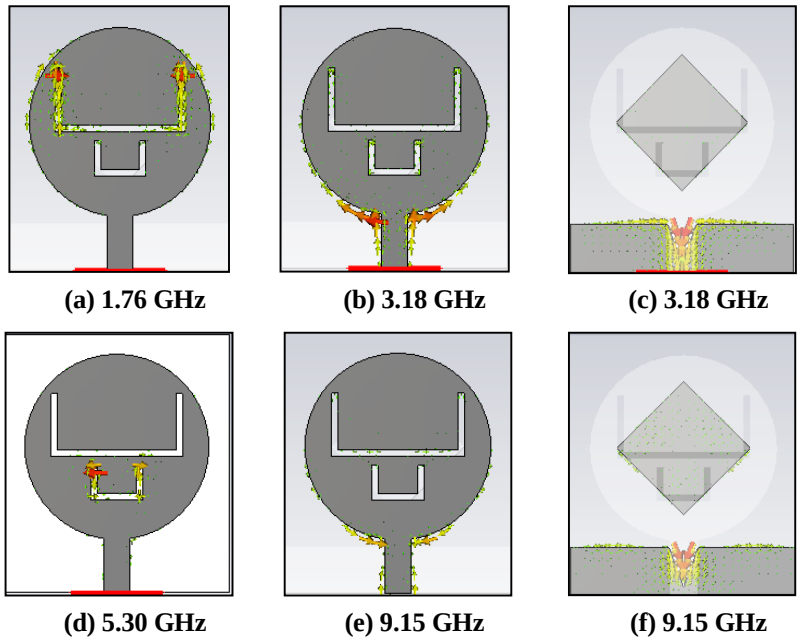

Fig. 9. Simulated surface current distributions of the modified structure at various frequencies.

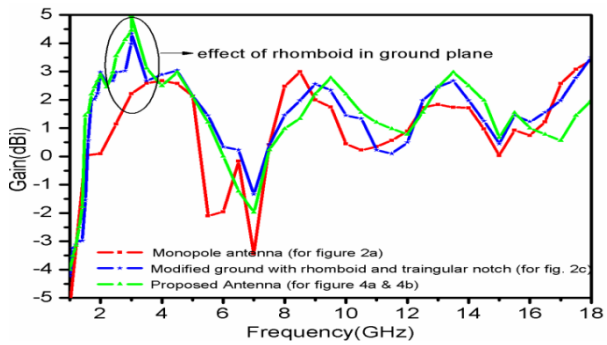

Fig. 10. Simulated variation of gain with frequency in three different cases.

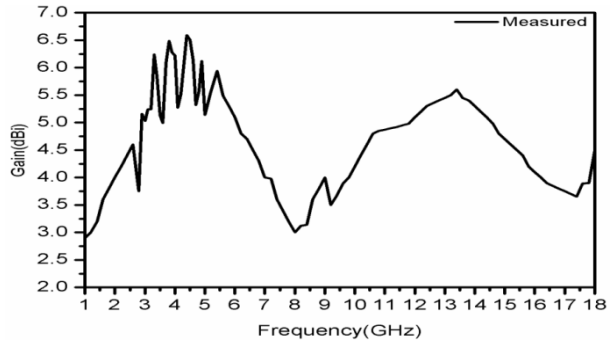

Fig. 11. Variation of measured gain with frequency of proposed structure.

The measured two dimensional co-polar and cross-polar radiation patterns in elevation and azimuth planes at three frequencies namely 1.76 GHz, 3.18 GHz and 9.15 GHz are shown in Figs. 12(a) to (f). It is realized that these two dimensional radiation patterns are nearly omni-directional in nature and significantly resembles with those of a monopole antenna operating under similar conditions. In elevation plane; the co-polar patterns at all frequencies are nearly 10 dB higher than cross-polar patterns while in azimuth plane, at all frequencies; co-polar patterns are nearly 15 dB higher than cross-polar patterns. The normalized radiation patterns of this structure are calculated through following equations:

$$E_{elevation} = [\, J_{n+1}(k_0 R \sin\theta) - J_{n-1}(k_0 R \sin\theta)] \cos n\phi \tag{8}$$

$$E_{Azimuth} = [\, J_{n+1}(k_0 R \sin\theta) + J_{n-1}(k_0 R \sin\theta)] \cos\theta \sin n\phi \tag{9}$$

where J_{n+1} and J_{n-1} are the Bessel functions of order n + 1 and n –1, θ is the elevation angle and ϕ is the azimuth angle.

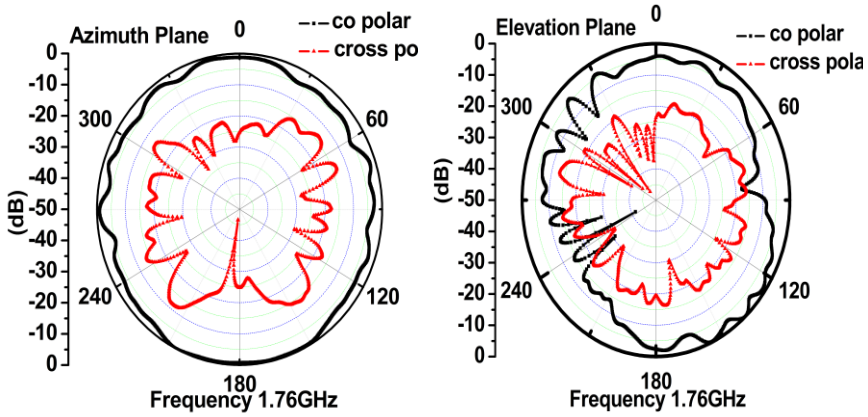

(a) 1.76 GHz **(b) 1.76 GHz**

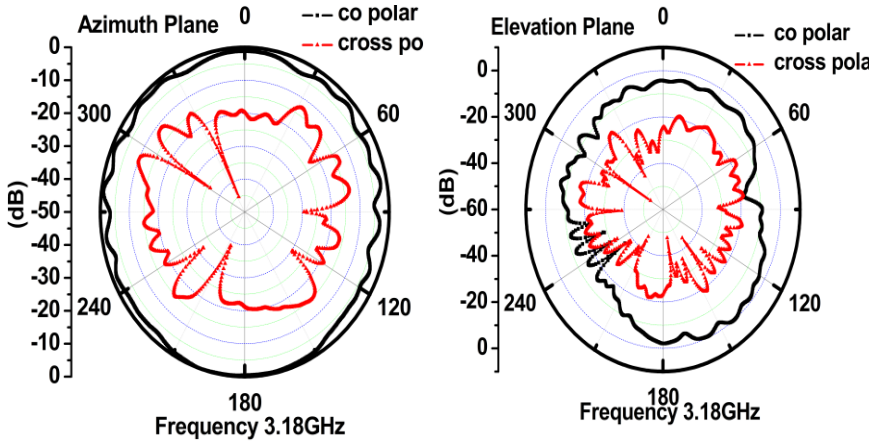

(c) 3.18 GHz **(d) 3.18 GHz**

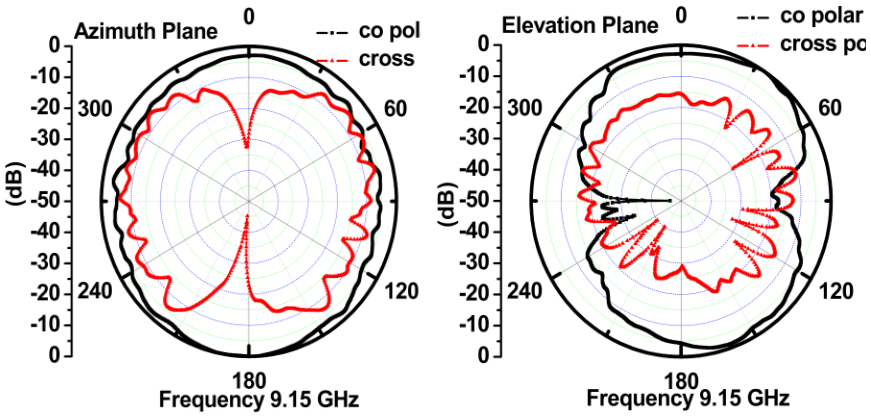

(e) 9.15 GHz **(f) 9.15 GHz**

Fig. 12. Measured 2-D radiation patterns in elevation (E-plane) and azimuth (H-Plane) planes at different resonance frequencies.

The polarization of proposed design has performed at several (θ, ϕ) values and finally with θ= 50° & ϕ= 74°, the best performance of the antenna is achieved. The simulated variation of axial ratio as a function of frequency is shown in Fig. 13. It indicates that antenna is presenting circular polarization in the frequency range 4.12 GHz to 5.20 GHz with axial ratio bandwidth close to 1.08 GHz.

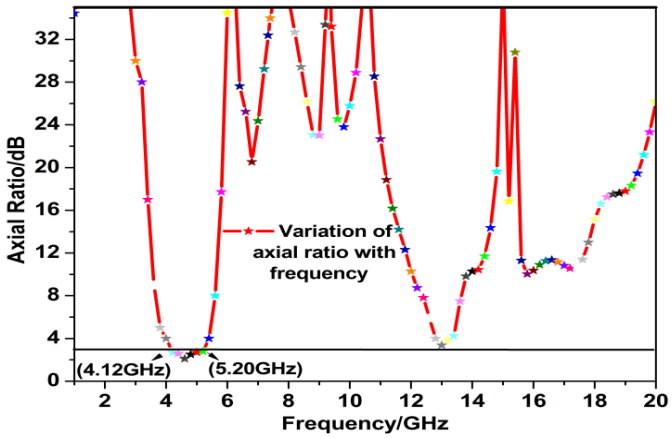

Fig. 13. Simulated variation of axial ratio with frequency.

The numerical simulation of the SAR values has evaluated on Specific Anthropomorphic Mannequin phantom head through CST Simulation program. This head is modelled by a shell filled with a liquid, which represent the average material properties of the head. The SAR values averaged over 1g biological tissue and are obtained by selecting IEEE standard [25]. The simulated power 0.5 W has used and SAR calculation performed in the post processing phase of the simulation. Figure 14 shows the geometry of the SAM model with proposed antenna.

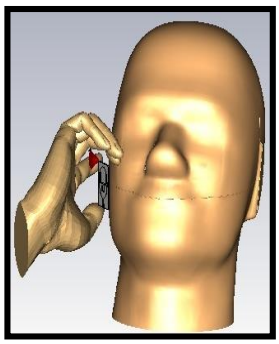

Fig. 14. Geometry of SAM Head Hand model with proposed antenna.

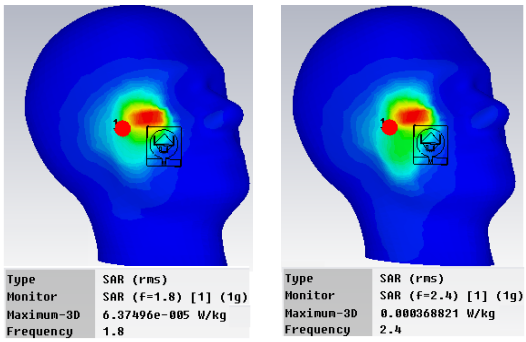

(a) 1.8 GHz **(b) 2.4 GHz**

Fig. 15. SAR values at different frequencies.

The effect of the human head on SAR values has studied at 1.8 GHz and 2.4 GHz, which is depicted in Fig. 15. The SAR values at 1.8 GHz is 0.000063749 W/kg and at 2.4 GHz is 0.00036884 W/kg for 1 gram of tissue on two frequency which are well interior the value specified by the FCC (1.6 W/kg). The proposed antenna acquired lower SAR values in the human head than that of a dipole and helical antenna.

4. Conclusions

This paper provides design and performance of a U-shaped slots loaded patch structure with modified ground plane through simulation and measured results. This antenna provides triple band performance with impedance bandwidths 157 MHz (in frequency range 1.733 to 1.89 GHz), 3.2 GHz (in frequency range 2.29 to 5.49 GHz) & 10.45 GHz (in frequency range 6.83 to 17.28 GHz), axial impedance bandwidth 1.08 GHz (in frequency range 4.12 GHz to 5.20 GHz), nearly flat gain (close to 6.5 dBi) and good radiation patterns and acceptable SAR value in the desired range. The maximum gain of the antenna is close to 6.59 dBi at 4.40 GHz. This antenna may be proved as a useful structure for modern radio communication systems including in Mobile and Bluetooth application, WLAN, WiMAX and UWB communication systems.

Acknowledgement

Authors are thankful to Department of Electronics & Information Technology, New Delhi and MHRD's DIC programme for providing financial support for the present work. Authors also extend their sincere thanks to Mr. V.V. Srinivasan, ISRO Satellite Centre, Bangalore and Mr. Fetah Lohar, Application Engineer, Jyoti Electronics for their valuable suggestions in this work.

References

1. Kumar, G.; and Ray, K.P. (2003). *Broadband microstrip antenna*. Massachusetts: Artech House.
2. Bahl, I.J.; and Bhartia, P. (1980). *Microstrip antennas*. Massachusetts: Artech House.

3. Chang, T.-H.; and Kiang, J.-F. (2013). Compact multi-band H-shaped slot antenna. *IEEE Transactions on Antennas and Propagation*, 61(8), 4345-4349.
4. Tang, H.; Wang, K; and Wu, R. (2017). Compact triple-band circularly polarized monopole antenna for WLAN and WiMAX application. *Microwave and Optical Technology Letters*, 59 (8), 1901-1908.
5. Chang, C.H.; Wei, W.C.; Ma, P.J.; and Huang, S. Y. (2013). Simple printed WWAN monopole slot antenna with parasitic shorted strips for slim mobile phone application. *Microwave and Optical Technology Letters*, 55(12), 2835-2841.
6. Mondal, K.; and Sarkar, P.P. (2017). Dual band compact monopole antenna for ISM 2.4/5.8 Frequency bands with bluetooth, wi-fi, and mobile applications. *Microwave and Optical Technology Letters*, 59(5), 1061-1065.
7. Liu, Y.T.; and Su, C.W. (2008). Wideband omni-directional operation monopole antenna. *Progress in Electromagnetics Research Letters*, 1, 255-261.
8. Malik; Patnaik, A.; and Kartikeyan, M.V.A. (2015). Compact dual band antenna with omnidirectional radiation pattern. *IEEE Antennas and Wireless Propagation Letters*, 14, 503-506.
9. Ray, K.P.; Thakur, S.S.; and Deshmukh R.A. (2012). Wideband L-shaped printed monopole antenna. *International Journal of Electronics & Communication*, 66(8), 693-696.
10. Yeo, W.L.; Lai, K.C.; Yeap, K.H.; Teh, P.C; and Nisar, H.A. (2017). A compact dual-band hook-shaped antenna for wireless application. Wideband L-shaped printed monopole antenna. *Microwave and Optical Technology Letters*, 59(8), 1882-1887.
11. Chitra, R.J.; and Nagarajan, V. (2013). Double L-slot microstrip patch antenna array for WIMAX and WLAN application. *Computers and Electrical Engineering*, 39, 1026-1041.
12. Beigi, P.; Nourinia, J.; Zehforoosh, Y.; and Mohammadi, B. (2015). A compact novel CPW-FED antenna with square spiral patch for multiband applications. *Microwave and Optical Technology Letters*, 57(1), 111-115.
13. Hsieh, D.H.; Wu, J.W.; Cheng, Y.W.; and Wang, C.J. (2015). A CPW fed meandered-shaped monopole antenna with asymmetrical ground planes. *Proceedings of the IEEE Radio and Wireless Symposium (RWS '15)*. San Diego, California, United States of America, 86-88.
14. Liu, P.; Zou, Y.; Xie, B.; Liu, X.; and Sun, B. (2012). Compact CPW fed tri-band printed antenna with meandering split-ring slot for WLAN/WiMAX applications. *IEEE Antennas and Wireless Propagation Letters*, 11, 1242-1244.
15. Pei; W., A.G.; Gao, S.; and Leng, W. (2011). Miniaturized triple-band antenna with a defected ground plane for WLAN/WiMAX applications. *IEEE Antennas and Wireless Propagation Letters*, 10, 298–301.
16. Deng, C.; Li, Y.; Zhang, Z.; and Feng, Z. (2015). Planar printed multi resonant antenna for octa-band WWAN/LTE mobile handset. *IEEE Antennas and Wireless Propagation Letters*, 14, 1734–1737.
17. Kim, D.O.; Kim, C.Y.; Yang, D.G.; and Ahmed, M.S. (2017). Multiband omnidirectional planar monopole antenna with two split ring resonator pairs. *Microwave and Optical Technology Letters*, 59(4), 753-758.

18. Guo, Z.; Tian, H.; Wang, X.; Luo, Q.; and Ji, Y. (2013). Bandwidth enhancement of monopole UWB antenna with new slots and EBG structures. *IEEE Antennas and Wireless Propagation Letters*, 12, 1550- 1553.
19. Goswami, S.A.; and Karia, D. (2017). A compact monopole antenna for wireless applications with enhanced bandwidth. *AEU-International Journal of Electronic and Communications*, 72, 33-39.
20. Neebha, T.M.; and Nesasudha M. (2016). Design and analysis of advanced microstrip patch antenna for endoscopic capsules. *Microwave and Optical Technology Letters*, 58(7), 1762-1767.
21. Simulia, D.S. (2014). Computer simulation technology. Retrieved May 10, 2016, from http://www.cst.com.
22. Balanis, C.A. (2005). *Antenna theory: Analysis & design* (3rd ed.). New York: John Wiley and Sons Inc.
23. Lin, C.C.; and Chuang, H.R. (2008). A 3-12 GHz UWB planar triangular monopole antenna with ridged ground-plane. *Progress in Electromagnetics Research*, 83, 307-321.
24. Ghalibafan, J.; Attari, A.R.; and Hojjat-Kashani, F. (2010). A new dual-band microstrip antenna with U-shaped slot. *Progress in Electromagnetics Research C*, 12, 215-223.
25. Means, D.L.; and Chan K.W. (2001). Evaluating compliance with Federal Communications Commision (FCC) guidelines for human exposure to radiofrequency electromagnetic fields. *FCC's Office of Engineering and Technology's World Wide Web*, OET bulletin 65, edition 97-01.